Laser-induced autoionization from a double Fano system

W. Leoński, R. Tanaś, and S. Kielich

Nonlinear Optics Division, Institute of Physics, Adam Mickiewicz University, 60-780 Poznań, Poland

Received January 28, 1986; accepted August 8, 1986

We discuss a system with two discrete levels embedded in one continuum, which, after Fano diagonalization, gives a double Fano profile with two zeros. The second zero, which is located between the two levels, does not disappear even when the asymmetry parameter q goes to infinity. The spectrum of photoelectrons from such a system is calculated for any strength of the exciting field.

INTRODUCTION

The past few years have witnessed a large growth of interest in research on laser-induced autoionization. A number of papers have appeared[1-17] that present various aspects of the problem, such as high-power line narrowing,[1-5] the effects of laser bandwidth, spontaneous emission and collisions,[6-10] resonance fluorescence from the autoionizing state,[11,12] excitation by smooth pulses,[13] and double-resonance effects.[14,15] Lambropoulos and Zoller[5] have studied autoionizing states in a strong laser field and noticed an interesting feature: the narrowing of the autoionizing resonance at a certain value of the field. This narrowing effect has been studied by Rzążewski and Eberly,[1] who called it a "confluence of coherences." They considered a simple, exactly solvable model consisting of a ground state, an autoionizing state, and the continuum. In a subsequent paper[6] they also included a finite laser bandwidth. Andryushin *et al.*[4] considered a model with two autoionizing states, mutually coupled by an intense laser field. Moreover, their model included transitions to the higher continuum states. Alber and Zoller[16] studied two-photon ionization into an autoionizing Rydberg series. They used the multichannel quantum defect theory to model the infinite number of autoionizing Rydberg states.

In this paper we consider a model with two closely lying autoionizing states of the same parity, both of which are coupled to the ground state by an intense laser field. The two autoionizing states are coupled also by the configuration mixing interaction to the same continuum. This model, which includes an additional autoionizing state, is an extension of the simple model of Rzążewski and Eberly.[1] From the standpoint of the atom alone, it is the Fano[18] model of "a number [two] of discrete states and one continuum" that can be diagonalized. The Fano diagonalization introduces a new eigenbasis of continuum states with some structure. In the case of two discrete states embedded in the continuum, this is a two-peak structure. This means that the weak-field absorption spectrum will be described by a Fano profile with two peaks and two zeros. We refer, in this paper, to such a profile as a double Fano profile. As Rzążewski and Eberly[1,6] have shown, the confluence of atomic and field coherences occurs whenever one of the Autler-Townes peaks, which are characteristic of any strong-field photoelectron spectrum, falls exactly on the zero of the Fano profile. Since there are two zeros in the double Fano profile that we consider here, some new possibilities arise. We explore some of these possibilities here. We briefly discuss the properties of the double Fano profile and concentrate next on the long-time photoelectron spectrum from such a system. The model admits of an exact, analytical solution, which we discuss extensively.

DOUBLE FANO PROFILE

The atomic model that we use in this paper is shown in Fig. 1. Besides the ground state $|0\rangle$, there are two discrete states $|1\rangle$ and $|2\rangle$ lying above the ionization threshold and interacting with the continuum by means of configurational (Coulombic) interaction. The two levels as well as the continuum are coupled to the ground state because of a strong laser beam of frequency ω_L. It is possible to obtain a fully analytical, nonperturbative solution to the problem even in the case of the double Fano profile (for perturbative solutions, see Ref. 19). This is our objective in this paper. We follow the path adopted by Rzążewski and Eberly.[1]

The Hamiltonian of the system can be written in the form (we use units $\hbar = 1$)

$$\hat{H} = \hat{H}_0 + \hat{H}_1 + \hat{H}_2 + \hat{H}_\omega + \hat{V}_{\text{Coul}} + \hat{V}_{\text{rad}}, \tag{1}$$

with the bare energies of the atom given by

$$\hat{H}_i = \omega_i |i\rangle\langle i|, \qquad i = 0, 1, 2, \tag{2a}$$

$$\hat{H}_\omega = \int d\omega \omega |\omega\rangle\langle\omega|. \tag{2b}$$

$\hat{V}_{\text{Coul}}$ describes the Coulombic configuration interaction and $\hat{V}_{\text{rad}} = -\mathbf{d}\cdot\mathbf{E}_L(t)$ the interaction of the atom with the laser light in the dipole and rotating-wave approximation. The laser field $\mathbf{E}_L(t)$ is treated classically. We also assume that $\omega_0 = 0$ for convenience. The following matrix elements describe the couplings between the bare atomic states:

$$V_1(\omega) = \langle 1|\hat{V}_{\text{Coul}}|\omega\rangle, \tag{3a}$$

$$V_2(\omega) = \langle 2|\hat{V}_{\text{Coul}}|\omega\rangle, \tag{3b}$$

$$V_{01} = \langle 0|\hat{V}_{\text{rad}}|1\rangle, \tag{3c}$$

$$V_{02} = \langle 0|\hat{V}_{\text{rad}}|2\rangle, \tag{3d}$$

$$V_0(\omega) = \langle 0|\hat{V}_{\text{rad}}|\omega\rangle. \tag{3e}$$

According to Fano, it is possible to diagonalize that part of the Hamiltonian expression (1) that includes configuration interaction, that is, $\hat{H}_L = \hat{H}_1 + \hat{H}_2 + \hat{H}_\omega + \hat{V}_{\text{Coul}}$. Introducing a new eigenbasis

0740-3224/87/010072-06$02.00

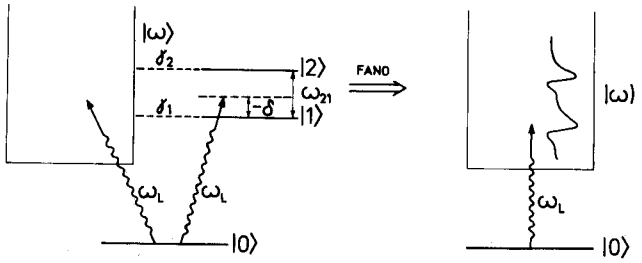

Fig. 1. Simplified atomic-level scheme. Configuration-interaction coupling of levels $|1\rangle$ and $|2\rangle$ to $|\omega\rangle$ leads to the double Fano continuum $|\omega\rangle$. This continuum is coupled to discrete state $|0\rangle$ by a laser of frequency ω_L.

$$\hat{H}_L|\omega) = \omega|\omega) \tag{4}$$

with eigenvectors $|\omega)$ denoted by round brackets, one can reexpress the radiation interaction energy in the form

$$\hat{V}_{\text{rad}} = \int d\omega\Omega(\omega)|0)(\omega| + H_L. \tag{5}$$

The matrix element $\Omega(\omega)$ describing the coupling of the ground state to the new, structured continuum is given by

$$\Omega(\omega) = V_0(\omega)e^{i\varphi} \times \frac{(\omega-\omega_1)(\omega-\omega_2)+\omega(q_1\gamma_1+q_2\gamma_2)-(\omega_1q_2\gamma_2+\omega_2q_1\gamma_1)}{(\omega-\omega_1)(\omega-\omega_2)-i\omega(\gamma_1+\gamma_2)+i(\omega_1\gamma_2+\omega_2\gamma_1)}, \tag{6}$$

where $V_0(\omega)$ is given by Eq. (3e) and ω_1 and ω_2 are the bare energies of the discrete atomic states given by Eq.(2a). The parameters γ_1, q_1 (γ_2, q_2) describe the autoionization linewidth and the Fano asymmetry parameter for the level $|1\rangle$ ($|2\rangle$). The phase φ is arbitrary. The absolute square of this matrix element $|\Omega(\omega)|^2$ is in fact what we refer to as the double Fano profile. We assume here, as is usually done, that $V_0(\omega)$ does not depend strongly on ω. This Fano profile describes the absorption spectrum of weak laser light when there are two closely lying autoionizing states that contribute to the spectrum. The shape of the double Fano profile is illustrated in Fig. 2 for different values of the parameters. The profile has two zeros, which are the two zeros of the numerator of Eq. (6). Their positions are

$$\omega = \frac{\omega_1 - q_1\gamma_1 + \omega_2 - q_2\gamma_2}{2} \pm \tfrac{1}{2}[\omega_{21}^2 + (q_1\gamma_1+q_2\gamma_2)^2 - 2\omega_{21}(q_2\gamma_2 - q_1\gamma_1)]^{1/2}, \tag{7}$$

where $\omega_{21} = \omega_2 - \omega_1$. Obviously, the positions of the zeros are shifted with respect to the Fano zero of a single autoionizing state, $\omega = \omega_1 - q_1\gamma_1$ or $\omega = \omega_2 - q_2\gamma_2$. In the degenerate case $\omega_2 = \omega_1$ ($\omega_{21} = 0$) the double Fano profile has only one zero for $\omega = \omega_1 - (q_1\gamma_1 + q_2\gamma_2)$ because the other zero $\omega = \omega_1$ is reduced by its counterpart in the denominator. On introducing the total autoionization rate $\Gamma = \gamma_1 + \gamma_2$ and the effective asymmetry parameter $Q = (q_1\gamma_1 + q_2\gamma_2)/\Gamma$, we have the well-known situation for a single autoionizing state characterized by Γ and Q. Generally, however, the double Fano profile has two zeros [given by Eq. (7)] as well as two peaks, as is evident from Fig. 2.

On defining the effective Rabi frequency of the interaction[6]

$$\Omega_0 \equiv \sqrt{4\pi\Gamma}(Q+i)V_0(\omega)e^{i\varphi}, \tag{8}$$

Eq. (6) can be transformed into

$$\Omega(\omega) = \frac{\Omega_0}{\sqrt{4\pi\Gamma}}\left(\frac{A_+}{\omega-\omega_+} + \frac{A_-}{\omega-\omega_-} + \frac{1}{Q+i}\right), \tag{9}$$

where $\omega_\pm$ are the complex roots of the denominator of Eq. (6) given by

$$\omega_\pm = \frac{\omega_1+\omega_2 \pm \nu}{2} + i\frac{\Gamma \pm \eta}{2}, \tag{10}$$

with

$$\eta = \frac{1}{\sqrt{2}}\{[(\omega_{21}^2-\Gamma^2)^2 + 4\omega_{21}^2(\gamma_2-\gamma_1)^2]^{1/2} - \omega_{21}^2 + \Gamma^2\}^{1/2},$$

$$\nu = \frac{1}{\sqrt{2}}\{[(\omega_{21}^2-\Gamma^2)^2 + 4\omega_{21}^2(\gamma_2-\gamma_1)^2]^{1/2} + \omega_{21}^2 - \Gamma^2\}^{1/2}. \tag{11}$$

The sign of η is the same as that of $\omega_{21}(\gamma_2 - \gamma_1)$. The complex amplitudes $A_\pm$ are given by the following expression:

$$A_\pm = \frac{\Gamma}{2}\left(1 \pm \frac{\omega_{21}\kappa + i\Gamma}{\nu + i\eta}\right), \tag{12}$$

where

$$\kappa = \frac{q_2\gamma_2 - q_1\gamma_1 + i(\gamma_2-\gamma_1)}{\Gamma(Q+i)}. \tag{13}$$

On an appropriate choice of φ, the Rabi frequency Ω_0 can be made real.

The form [Eq. (9)] of the radiative matrix element $\Omega(\omega)$ is a generalization of the corresponding formula of Rzążewski and Eberly[1] to the case of two autoionizing levels, both of which are radiatively coupled to the ground state. Equation (9) shows explicitly the resonant structure of the radiative

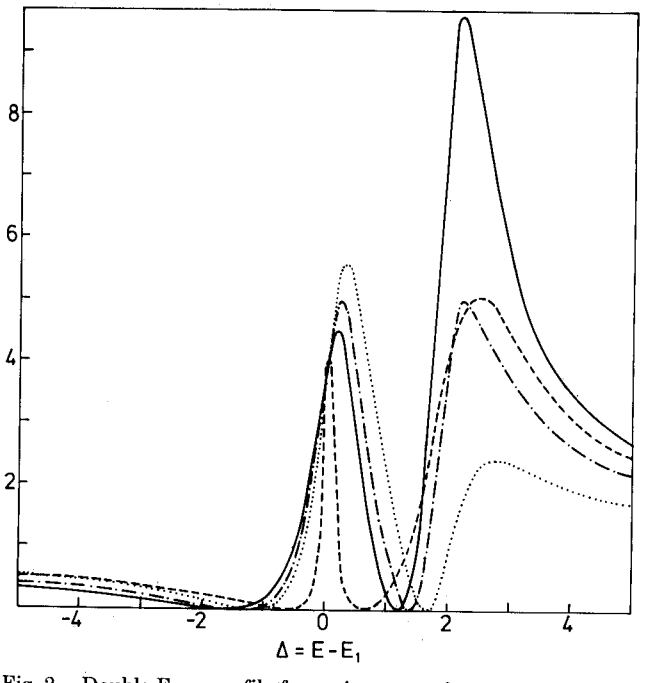

Fig. 2. Double Fano profile for various sets of parameters. Solid line: $\gamma_1 = \gamma_2 = 0.5, q_1 = 2, q_2 = 3$. Dotted line: $\gamma_1 = \gamma_2 = 0.5, q_1 = 2, q_2 = 1$. Dashed–dotted line: $\gamma_1 = \gamma_2 = 0.5, q_1 = q_2 = 2$. Dashed line: $\gamma_1 = 0.1, \gamma_2 = 0.9, q_1 = q_2 = 2$. The separation of the two levels $\omega_{21} = 2$.

coupling. It is a superposition of two Lorentzians and a flat background. So in the case of the double Fano profile we have one extra Lorentzian, which is due to the presence of an extra autoionizing state. The flat background can be replaced by a broad Lorentzian[6]; this will prove highly convenient in our further calculations, making the model considered here a three-Lorentzian model. Despite its complications, this model is still strictly solvable.

In the degenerate case, $\omega_{21} = 0$, we have $A_+ = \Gamma$, $A_- = 0$, and one of the Lorentzians disappears.

We shall use this model to calculate the steady-state spectrum of photoelectrons in a strong laser field.

PHOTOELECTRON SPECTRUM

Since we shall not be studying statistical effects such as laser linewidth and radiative relaxation,[6-10] we can use the exact state function to describe the evolution of the atom in a laser field.[1,5] The time-dependent Schrödinger wave vector can be written as

$$|\psi(t)\rangle = \alpha(t)|0\rangle + \int d\omega \beta_\omega(t)|\omega\rangle, \tag{14}$$

and the equations for the pure-state amplitudes $\alpha(t)$ and $\beta_\omega(t)$ are (in the rotating frame,[20] under the assumption of a step turn-on of the laser, and with $\omega_0 = 0$) as follows:

$$\dot{\alpha}(t) = -i \int d\omega \Omega(\omega)\beta_\omega(t), \tag{15a}$$

$$\dot{\beta}_\omega(t) = -i(\omega - \omega_L)\beta_\omega(t) - i\Omega^*(\omega)\alpha(t). \tag{15b}$$

Although Eqs. (15a) and (15b) are of the same form as those of Rzążewski and Eberly, they differ in one important point: the form of $\Omega(\omega)$. In our case $\Omega(\omega)$ describes what we call the double Fano profile and is given by Eq. (6) or (9).

Using the standard procedure of Laplace transforms with the initial conditions $\alpha(0) = 1$, $\beta_\omega(t) = 0$, the system of Eqs. (15a) and (15b) goes over into a system of algebraic equations in the Laplace-transformed variables $\tilde{\alpha}(z)$ and $\tilde{\beta}_\omega(z)$ and can be easily solved for the transformed variables. Our aim in this paper is to calculate the long-time-limit spectrum of photoelectrons in the case of two interfering autoionizing states, i.e.,

$$W(\omega) = \lim_{t\to\infty} |\beta_\omega(t)|^2. \tag{16}$$

Likewise, in the case of a single autoionizing state, a fully analytical, explicit formula for the spectrum of photoelectrons can be obtained. This formula has the form

$$W(\omega) = \left| \frac{\Omega(\omega)}{G[z = -i(\omega - \omega_L)]} \right|^2, \tag{17}$$

where

$$G(z) = \frac{1}{\tilde{\alpha}(z)} = z + \int d\omega \frac{|\Omega(\omega)|^2}{z + i(\omega - \omega_L)}. \tag{18}$$

By using the explicit form of $\Omega(\omega)$ given by Eq. (9), the integrations in Eq. (18) can be performed explicitly. We assume in our calculations that both autoionizing levels lie far above the ionization edge, and we neglect any edge effects. We also use the procedure[1] consisting of the replacement of the flat background in $\Omega(\omega)$ by a Lorentzian, and after calculations we take the limit for the infinite width of this Lorentzian. This leads us to the following result:

$$G[z = -i(\omega - \omega_L)] = -i(\omega - \omega_L) - \frac{\Omega_0^2}{4\Gamma}\left(\frac{B_+}{\omega - \omega_+} + \frac{B_-}{\omega - \omega_-} + \frac{1}{Q^2 + 1} \right), \tag{19}$$

where

$$B_\pm = 2A_\pm \left[\frac{A_\pm^*}{i(\Gamma \pm \eta)} + \frac{A_\mp^*}{i\Gamma \pm \nu} + \frac{1}{Q - i} \right]. \tag{20}$$

All the other quantities occurring in Eqs. (19) and (20) have already been defined [Eqs. (10)–(13)]. It should be kept in mind that $\Gamma = \gamma_1 + \gamma_2$ means the total autoionization rate and $Q = (q_1\gamma_1 + q_2\gamma_2)/\Gamma$ is an effective asymmetry parameter.

On insertion of all these expressions into Eq. (17), one obtains an explicit, analytical formula describing the long-time photoelectron spectrum in terms of the atomic parameters γ_1, q_1, γ_2, q_2, ω_{21}, the laser frequency ω_L, and the Rabi frequency Ω_0.

This formula is valid for weak as well as for strong fields. In the degenerate case ($\omega_{21} = 0$) of two autoionizing levels with the same parameters ($\gamma_1 = \gamma_2$ and $q_1 = q_2$) we have $A_- = B_- = 0$, and our formula goes over into that of Rzążewski and Eberly.[1,6] It should be noted here, however, that even if $A_- \to 0$, B_- does not necessarily become zero because simultaneously $\eta \to \Gamma$ and $|A_-|^2/(\Gamma - \eta)$ can tend to a finite value. In fact, B_- is equal to zero only if the two levels are identical, i.e., if $\gamma_1 = \gamma_2$ and $q_1 = q_2$. This is an interesting feature of the photoelectron spectrum in the case of the double Fano profile.

As is obvious on inspection of formulas (11) and (13), the two collective parameters Γ and Q by no means suffice to describe the system; two more parameters are needed: $\Gamma_{21} = \gamma_2 - \gamma_1$ and $Q_{21} = (q_2\gamma_2 - q_1\gamma_1)/\Gamma$.

So, for the double Fano profile, the photoelectron spectrum formula is much more complicated than for the single Fano profile. Some features of the spectrum can nevertheless be anticipated from the structure of Eqs. (9) and (19). For example, from Eq. (19) it is clear that for weak fields ($\Omega_0/\Gamma \ll 1$) the elastic peak, $\omega = \omega_L$, will dominate the spectrum. As the intensity of laser light increases, however, the terms proportional to Ω_0^2 become more and more important and the shape of the spectrum is not easy to predict without numerical evaluation. We present here several pictures illustrating characteristic features of the photoelectron spectrum for various sets of atomic and field parameters. In all our graphs, we have used the convention in which the spectra are plotted against the parameter $\Delta = \omega - \omega_1$. This means that the location of the spectral peaks (and zeros) is given with respect to the position of the lower autoionizing level ($\Delta = 0$ is the position of this level). The position of the second, higher autoionizing level is given by the value of $\Delta = \omega_{21} = \omega_2 - \omega_1$. The laser frequency tuning is defined by the parameter $\delta = \omega_1 - \omega_L$, i.e., $\delta = 0$ means that the laser frequency ω_L is tuned exactly to the lower autoionizing level. All the frequencies (energies) are given in units of Γ.

In Fig. 3 the photoelectron spectrum for large q values is

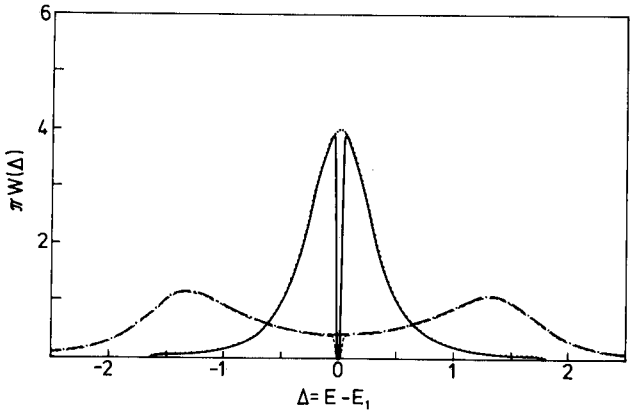

Fig. 3. Long-time photoelectron spectrum in the degenerate case $\omega_{21} = 0$ for two strengths of the field, $\Omega_0 = 1, 3$. The dotted and dashed–dotted lines are for the same asymmetry parameters $q_1 = q_2 = 100$, the solid and dashed lines for different q's: $q_1 = 90$, $q_2 = 100$. Autoionization widths are $\gamma_1 = \gamma_2 = 0.5$, and the laser is tuned to the lower level ($\delta = 0$).

presented in the degenerate case in which the two autoionizing states have the same energy.

For identical q values of the two autoionizing states $q_1 = q_2 = 100$ the spectrum exactly reproduces that obtained by Rzążewski and Eberly[6] (see their Fig. 10). For easier comparison we have taken Rabi frequency values identical to theirs.

For strong field $\Omega_0 = 3$ we get a symmetric Autler–Townes doublet, as expected, and there is no indication whatsoever that, in fact, two states contribute to the spectrum. If the levels have different asymmetry parameters ($q_1 = 90$, $q_2 = 100$), however, a sharp wedge in the spectrum appears in the vicinity of $\Delta = 0$. This is the effect of the zero that, in the double Fano profile, occurs for $\Delta = 0$. To be precise, for $\omega_{21} = 0$ in the double Fano profile given by Eq. (6) this zero is counteracted by the same zero in the denominator, and one obtains the single Fano profile. However, when the double Fano profile is used to calculate $G(z)$ according to Eq. (18) first, and the limit $\omega_{21} \to 0$ is taken next, this zero reappears in the spectrum. This is because the amplitude A_- of the additional Lorentzian in the double Fano profile given in the form of Eq. (9) does not tend to zero fast enough to counteract the zero for $\omega \to \omega_-$, and this additional Lorentzian contributes to $G(z)$. In other words, this is the situation when, for $A_- \to 0$, the value of $|A_-|^2/(\Gamma - \eta)$ remains different from zero, and we have $B_- \neq 0$ [see Eqs. (15) and (20)], which reintroduces the zero for $\omega \to \omega_-$ into the spectrum. So the existence of such a zero in the photoelectron spectrum would be an indication that the spectrum comes from two autoionizing states. For a weaker field ($\Omega_0 = 1$) the change in the spectrum is even more dramatic. However, the spectrum is affected only within a narrow range on either side of the additional zero beyond which the spectrum is unchanged. It will not be easy to observe this effect in experiment.

In Fig. 4 we again have the degenerate case $\omega_{21} = 0$, but in this case the photoelectron spectrum is plotted for small q values. Again we have a Rzążewski-Eberly spectrum if $q_1 = q_2$. In a strong field ($\Omega_0 = 3$), the confluence-of-coherences effect is clearly visible. In the case of different q values the second zero at $\Delta = 0$ occurs, as in Fig. 3. Beyond this point the spectrum changes only slightly as long as the q's do not change considerably. Of course, the zero under discussion would not occur in the spectrum had we first taken the limit $\omega_{21} \to 0$ in the Fano profile and next performed the integrations leading to the formula for $G(z)$.

In the nondegenerate case, if the two autoionizing levels have different energies ($\omega_{21} \neq 0$), the double Fano profile is a two-peak profile the shape of which is dependent on the autoionization widths γ_1 and γ_2 and the asymmetry parameters q_1 and q_2, as seen in Fig. 2. Several characteristic features of the photoelectron spectrum obtained with such a profile are illustrated in Figs. 5–8. In Fig. 5 some examples of the spectrum are given for autoionizing states with the same width, i.e., $\gamma_1 = \gamma_2$, but different q's. In the case when $q_1 = 2$ and $q_2 = 10$, the spectrum is quite similar to the single-autoionizing-level case with narrowing of the left-hand Autler–Townes peak owing to the confluence of coherences effect. It has an extra zero for $\Delta = 0.45$, which does not affect the shape of the spectrum much because the spectrum has its minimum close to this zero.

In this case, the existence of the second autoionizing level has only a minor effect on the photoelectron spectrum. The situation changes dramatically when this zero moves to the right and becomes closer to the right-hand Autler–Townes peak. In this case the conditions for the confluence of coherences are satisfied for both Autler–Townes peaks, and we obtain a narrowing of the two peaks. This tendency is shown clearly by the curves for $q_1 = q_2 = 2$ with zero for $\Delta = 1.41$, and for $q_1 = 10$, $q_2 = 2$ with zero for $\Delta = 1.74$. In Fig. 6 the same spectrum is shown but for essentially different autoionizing widths of the levels $\gamma_1 = 0.1$ and $\gamma_2 = 0.9$. The locations of the zeros are as follows: for $q_1 = 2$ and $q_2 = 10$, $\Delta = -7.26, 0.06$; for $q_1 = q_2 = 2$, $\Delta = -0.63, 0.63$; for $q_1 = 10$ and $q_2 = 2$, $\Delta = -1.87, 1.07$. The line narrowing is clearly visible in the figure.

In the case of large q values one of the two zeros shifts far away toward negative values of Δ and ceases to affect the spectrum. The second zero, however, always remains some-

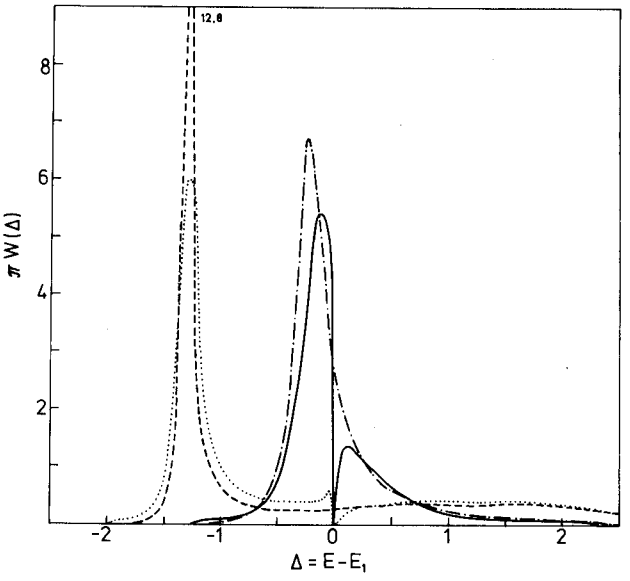

Fig. 4. Same as Fig. 3 but for small q values. Dashed–dotted and dashed lines, $q_1 = q_2 = 2$; solid and dotted lines, $q_1 = 2$, $q_2 = 3$.

where between the two autoionizing levels, as is evident from Eq. (7). This zero can still affect the spectrum. The effect of this zero on the strong-field ($\Omega_0 = 3$) photoelectron spectrum is illustrated in Figs. 7 and 8. In Fig. 7 the spectrum is shown for $q_1 = q_2 = 100$ and various separations of the two autoionizing states. For $\omega_{21} = 0$ we have the degenerate case, and the spectrum is identical to that of Rzążewski and Eberly.[6] If the two levels are far apart ($\omega_{21} = 10$), the influence of the second level disappears. We recall that the laser is tuned exactly to the lower autoionizing level ($\delta = 0$), and (for $\Omega_0 = 3$) the zero is located to the right of the Autler–Townes doublet. In this case, we have a regular Autler–Townes doublet but with the width $\gamma_1 = 0.5$ (instead of $\Gamma = 1$) because only the lower level contributes to the spectrum. In the intermediate case $\omega_{21} = 1.5$ the spectrum is essentially

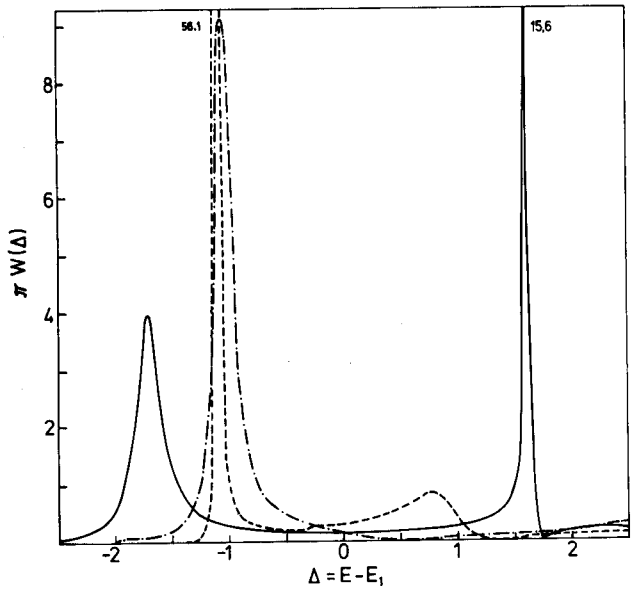

Fig. 5. Strong-field ($\Omega_0 = 3$) photoelectron spectrum for the nondegenerate case $\omega_{21} = 2$, $\gamma_1 = \gamma_2 = 0.5$, $\delta = 0$. Dashed line, $q_1 = q_2 = 2$; dashed–dotted line, $q_1 = 2$, $q_2 = 10$; solid line $q_1 = 10$, $q_2 = 2$.

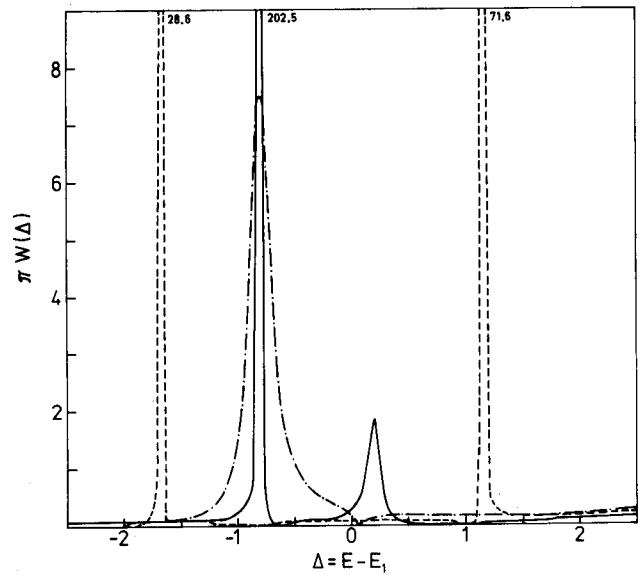

Fig. 6. Same as Fig. 5 but for different widths $\gamma_1 = 0.1$, $\gamma_2 = 0.9$. Solid line, $q_1 = q_2 = 2$; dashed line, $q_1 = 10$, $q_2 = 2$; dashed–dotted line, $q_1 = 2$, $q_2 = 10$.

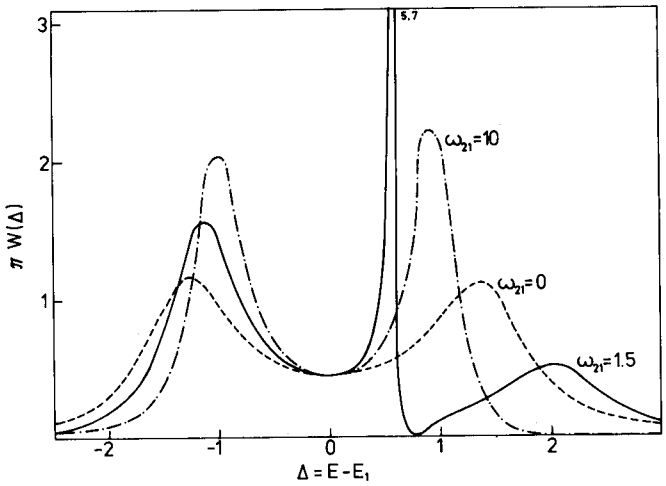

Fig. 7. Strong-field photoelectron spectrum for large asymmetry parameters $q_1 = q_2 = 100$ and various separations of the levels; $\gamma_1 = \gamma_2 = 0.5$, $\delta = 0$, $\Omega_0 = 3$.

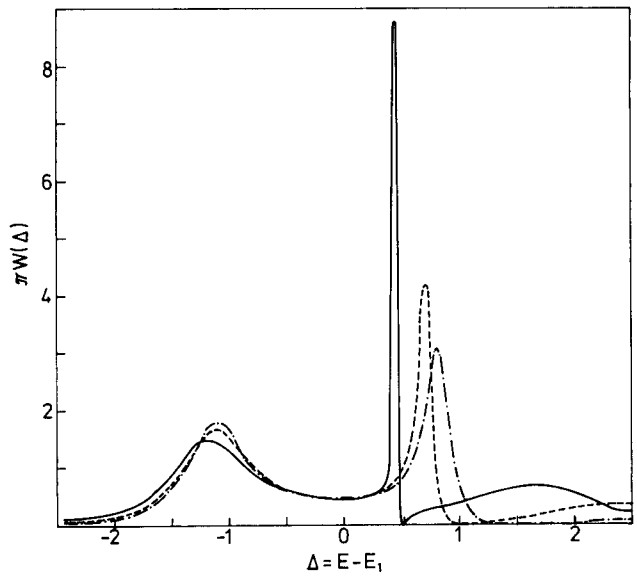

Fig. 8. Same as Fig. 7 but for other level separations. Solid line, $\omega_{21} = 1.01$; dashed line, $\omega_{21} = 2$; dashed–dotted line, $\omega_{21} = 3$.

distorted; a very narrow peak accompanied by a zero is clearly visible. Incidentally, $\omega_{21} = 1.5$ means that the Autler–Townes peak occurs at the position of the second level. This fact is of no great significance, as we note from Fig. 8, where the spectrum is presented for values of ω_{21} equal to 1, 2, and 3. For $\omega_{21} = 3$ the interlevel zero of the double Fano profile is located at $\Delta = 1.5$ and the condition for the confluence of coherences is satisfied. Narrowing of the right-hand Autler–Townes peak does occur, as one would expect, but the left-hand peak remains almost unchanged. The confluence-of-coherences effect in this case takes on a different appearance from that discussed earlier.

CONCLUSIONS

We have investigated the problem of laser-induced autoionization from a system with two closely lying autoionizing states that are both coupled to the ground state by the laser

field. A Fano diagonalization, leading to a double Fano profile with two peaks and two zeros, can be performed for such a system. We have briefly discussed the properties of such a double Fano profile. Since the roots of the polynomials in the numerator and the denominator of this profile can be found explicitly, the profile can be written as a superposition of two Lorentzians and a flat background. This model, involving an additional Lorentzian compared with the model considered by Rzążewski and Eberly, is, nevertheless, tractable in the same manner. It permits an exact, analytical formula to be obtained for the long-time photoelectron spectrum. We have derived such a formula and have discussed the properties of the spectrum for strong exciting fields. Special attention has been paid to the locations of the two zeros of the double Fano profile, which are of basic importance in determining the shape of the photoelectron spectrum. Since the positions of the zeros are dependent on the parameters of both autoionizing states, the resulting spectrum is not a simple superposition of spectra from two individual autoionizing states but reflects an interference between the two. Another interference effect, i.e., interference between atomic and laser coherences leading to the confluence-of-coherences effect, is also apparent in the spectrum. The spectrum for various autoionization widths and asymmetry parameters of the levels is presented graphically for degenerate as well as nondegenerate cases.

The existence of two zeros in our photoelectron spectrum is reminiscent of a similar feature of the spectrum obtained by Deng and Eberly,[15] who considered double-resonance effects in strong-field autoionization. In their model, however, one Fano continuum is coupled to two different discrete levels by two lasers of different frequencies.

We should also emphasize that in order to make our model as simple as possible we have neglected some physical processes that can affect the photoelectron spectrum in an essential way. It has been shown, for example, by Andryushin *et al.*[21] that the photoionizing transitions to the higher continuum states may be important in some physical situations and may modify dramatically the photoelectron spectrum. They may even completely wash away the confluence-of-coherences effect, which is clearly visible in our simplified model. We believe, however, that our model, despite its simplicity, describes some essential features of the photoelectron spectrum that arise because of interference of the two adjacent autoionizing states.

ACKNOWLEDGMENT

This research was supported by the Research Project CPBP 01.07.

REFERENCES

1. K. Rzążewski and J. H. Eberly, Phys. Rev. Lett. **47,** 408 (1981), and references cited therein.
2. L. Armstrong, Jr., B. L. Beers, and S. Feneuille, Phys. Rev. A **12,** 1903 (1975).
3. Yu. I. Heller and A. K. Popov, Opt. Commun. **18,** 449 (1976); Yu. I. Heller, V. F. Lukinykh, A. K. Popov, and V. V. Slabko, Phys. Lett. A **82,** 4 (1981).
4. A. I. Andryushin, A. E. Kazakov, and M. V. Fedorov, Zh. Eksp. Teor. Fiz. **82,** 91 (1982) [Sov. Phys. JETP **55,** 53 (1982)]; A. I. Andryushin, M. V. Fedorov, and A. E. Kazakov, J. Phys. B **15,** 2851 (1982).
5. P. Lambropoulos and P. Zoller, Phys. Rev. A **24,** 379 (1981).
6. K. Rzążewski and J. H. Eberly, Phys. Rev. A **27,** 2026 (1983).
7. J. H. Eberly, K. Rzążewski, and D. Agassi, Phys. Rev. Lett. **49,** 693 (1982); D. Agassi, K. Rzążewski, and J. H. Eberly, Phys. Rev. A **28,** 3648 (1983).
8. G. S. Agarwal, S. L. Haan, K. Burnett, and J. Cooper, Phys. Rev. Lett. **48,** 1164 (1982); Phys. Rev. A **26,** 2277 (1982); G. S. Agarwal, S. L. Haan, and J. Cooper, Phys. Rev. A **29,** 2552, 2565 (1984).
9. G. S. Agarwal and D. Agassi, Phys. Rev. A **27,** 2254 (1983).
10. A. M. Lewenstein, J. W. Haus, and K. Rzążewski, Phys. Rev. Lett. **50,** 417 (1983); J. W. Haus, M. Lewenstein, and K. Rzążewski, Phys. Rev. A **28,** 2269 (1983); J. Opt. Soc. Am. B **1,** 641 (1984).
11. L. Armstrong, Jr., C. E. Theodosiou, and M. J. Wall, Phys. Rev. A **18,** 2538 (1978).
12. M. Crance and L. Armstrong, J. Phys. B **15,** 3199 (1982).
13. K. Rzążewski, Phys. Rev. A **28,** 2565 (1983).
14. P. E. Coleman and P. L. Knight, J. Phys. B **14,** 2139 (1981).
15. Z. Deng and J. H. Eberly, J. Opt. Soc. Am. B **1,** 102 (1984).
16. G. Alber and P. Zoller, Phys. Rev. A **29,** 2290 (1984).
17. Y. S. Kim and P. Lambropoulos, Phys. Rev. A **29,** 3159 (1984).
18. U. Fano, Phys. Rev. **124,** 1866 (1961).
19. S. Kielich, Acta Phys. Polon. **30,** 393 (1966), and references cited therein.
20. See, for instance L. Allen and J. H. Eberly, *Optical Resonance and Two-Level Atoms* (Wiley, New York, 1975).
21. A. I. Andryushin, A. E. Kazakov, and M. V. Fedorov, Zh. Eksp. Teor. Fiz. **88,** 1153 (1985) [Sov. Phys. JETP **61,** 678 (1985)].